Egyptian Journal of Chemistry

http://ejchem.journals.ekb.eg/

Novel Cationic Gemini Surfactant as a Corrosion Inhibitor for Carbon Steel Tubes during the Pickling Process: Synthesis, Surface Properties and Adsorption Behavior

A.S. El-Tabei[a], M.A. Hegazy[a,*], A.H. Bedair[b], M.A. Sadeq[b]

[b] *Faculty of Science, Azhar Univ., Chemistry Dept., Nasr City, Cairo, Egypt*

[a] *Egyptian Petroleum Research Institute (EPRI), Nasr City, Cairo, Egypt*

Abstract

Synthesis, surface parameters and corrosion inhibition efficiency (η) of novel cationic gemini surfactant (NCGSN) (namely: *N,N'*-(((2,2'-(naphthalene-1,5-diylbis(oxy))bis(acetyl))bis(oxy))bis(propane-3,1-diyl))bis(*N,N*-dimethyldodecan-1-aminium)dibromide were studied and discussed. The η of carbon steel (CS) was determined by weight loss (WL), electrochemical impedance spectroscopy (EIS) & potentiodynamic polarization (PP) in the absence and presence of NCGSN. The η and charge transfer resistance (R_{ct}) increases with increasing the NCGSN concentration and decreases with increasing the temperature. Kinetic and adsorption thermodynamic values showed that the η occurs through adsorption of NCGSN molecules on CS surface according to Langmuir isotherm. The PP results proposed the NCGSN regards a mixed-type inhibitor. Chemical and electrochemical results confirmed by SEM and EDX results which recommended the NCGSN adsorption occurs due to the barrier film formed on CS surface.

***Key words*:** Carbon steel; Surfactant; Acid inhibition; Weight loss; EIS; Tafel; SEM; EDX.

1. Introduction

The cationic gemini surfactants have the ability to be adsorbed on the metal-surface and form an adsorbed film that acts as a barrier between CS surface and corrosive materials like acidic solutions **[1-5]**, this adsorption may occur as a chemical adsorption or physical adsorption or both.

Many industrial processes that occur at elevated temperatures leave a thin oxide film or scale on the surface. Pickling or acid cleaning regards a metal cleaning process that is used to eliminate undesired layers, such as rust or scale which formed during industrial processes **[6]**. Pickle liquid or cleaning solution usually contains acid such as HCl and H_2SO_4 which are common, but its other different applications use various other acids as H_3PO_4, HNO_3, HF, sulfamic, citric, oxalic, … etc. or alkaline solution can be used to remove the surface impurities, scale or clean metal in various metal manufacturing processes **[7]**. Some additives such as wetting agents and corrosion inhibitors must be added to the pickle liquor **[8]**. In pickling process, HCl is the common acid although it is more expensive than H_2SO_4, as it is much faster and minimizes the metal loss **[9]**. Steels contain an alloy content less than or equal to 6%, are often pickled in HCl or H_2SO_4 while steels contain an alloy content greater than 6% must be pickled in two steps and acids such as H_3PO_4, HNO_3 and HF are preferred **[10]**.

In this study, we synthesize and investigate the surface properties, adsorption and inhibition behaviour of novel cationic gemini surfactant (NCGSN) (namely: *N,N'*-(((2,2'-(naphthalene-1,5-

Corresponding author Tel: +20 10 02653529; Fax: +20 2 22747433
E-mail address: mohamed_hgazy@yahoo.com (M.A. Hegazy)
Receive Date: 09 February 2020, Revise Date: 15 February 2020, Accept Date: 16 February 2020
DOI: 10.21608/EJCHEM.2020.23774.2413
©2020 National Information and Documentation Center (NIDOC)

diylbis(oxy))bis(acetyl))bis(oxy))bis(propane-3,1-diyl))bis(*N*,*N*-dimethyldodecan-1-aminium)dibromide as corrosion inhibitor for CS tubes during pickling process. Corrosion behavior of CS in 5% HCl has been studied using WL, EIS and PP with and without NCGSN. The adsorption mechanism of NCGSN is discussed through chemical structure, adsorption isotherm and thermodynamic parameters. Surface morphology of CS was studied by SEM & EDIX.

2. Experimental

2.1. Synthesis

2.1.1. Synthesis of Diethyl 2,2'-(naphthalene-1,5-diylbis(oxy))diacetate (I)

1,5-Dihydroxy naphthalene (0.8 g, 5 mmol), ethyl chloroacetate (1.34 g, 11 mmol) and anhydrous potassium carbonate (1.66 g, 12 mmol) were mixed in a round bottom flask with dry acetone (50 ml). The reaction mixture was stirred for 8 h at 60 ºC. After completion, the reaction mixture was filtered and the solvent was removed. The isolated product was washed with sodium hydroxide (5%, 5 ml) solution and water then the product was extracted with (25 ml) dichloromethane. The organic extract was collected and dried over anhydrous sodium sulfate. Subsequent removal of solvent gave the desired ester. Isolated yield: 91%. Mp: 120-122 ºC.

2.1.2. Synthesis of 2,2'-(Naphthalene-1,5-diylbis(oxy))diacetic acid (II)

The above product (Diethyl 2,2'-(naphthalene-1,5-diylbis(oxy))diacetate) (1.66 g, 5 mmol) and sodium hydroxide (0.48 g, 12 mmol) were dissolved in mixed solvent methanol: water (4:1, 20 ml) and refluxed for one hour at 65 ºC. After completing the reaction, the solvent was removed, then (30 ml) of water was added to it and the solution was acidified with diluted hydrochloric acid (20 ml, 10%). The solid product was isolated and further purified by recrystallizing from methanol. Isolated yield: 89%. Mp: over 300 ºC.

2.1.3. Synthesis of bis(3-(dimethylamino)propyl) 2,2'-(naphthalene-1,5-diylbis(oxy))diacetate (III)

2,2'-(Naphthalene-1,5-diylbis(oxy))diacetic acid (0.552 g, 2 mmol), 3-(dimethylamino)propan-1-ol (0.412 g, 4 mmol) and *p*-toluenesulfonic acid (2%) were mixed in a round bottom flask with dry xylene (100 ml), the flask was fitted with Dean-stark trap and condenser. The reaction mixture was stirred at 150 ºC until the theoretical amount of water was collected and then cooled to room temperature. After completing the reaction, the solvent was removed till dryness; the oily product was washed several times with dry diethyl ether.

2.1.4. Synthesis of *N*,*N'*-(((2,2'-(naphthalene-1,5-diylbis(oxy))bis(acetyl))bis(oxy))bis(propane-3,1-diyl))bis(*N*,*N*-dimethyldodecan-1-aminium)dibromide (IV)

A mixture of bis(3-(dimethylamino)propyl) 2,2'-(naphthalene-1,5-diylbis(oxy))diacetate (0.44 g, 1 mmol) and 1-bromododecane (0.496 g, 2 mmol) in ethanol was refluxed for 48 h to produce the quaternary product. The mixture was allowed to cool and the obtained light yellow precipitate was further purified by diethyl ether, dioxane then recrystallized from ethanol.

The scheme of the novel synthesized cationic gemini surfactant (NCGSN) is shown in **Fig. 1**.

The confirmation of the chemical structure of NCGSN had been done by different techniques such as FTIR, ^{1}H-NMR and mass spectroscopies.

2.2. Carbon steel

The CS specimens have the following composition (wt.%): 0.19% C, 0.014% Ni, 0.009% Cr, 0.022% Cu, 0.05% Si, 0.94% Mn, 0.009% P, 0.004% S, 0.034% Al, 0.016% V, 0.003% Ti and the rest Fe. They were abraded by emery papers with different grades (600–1200) and cleaned with acetone and distilled water.

2.3. Surface tension measurements

Surface tension experiments were carried out as previously described **[3-5]**.

2.4. Weight loss technique

The CS specimens have dimensions (2 cm × 4 cm × 0.5 cm) and immersed in 5% HCl solution for 24 hours in the absence and presence of various concentrations of NCGSN then the weight loss was measured and reported.

2.5. Electrochemical techniques

The electrochemical curves were documented by a Voltalab 40 Potentiostat PGZ 301 and a private computer provided with Voltamaster 4 software at 25 ºC. Electrochemical cell contains a platinum counter electrode (CE) and a saturated calomel electrode (SCE) as a reference electrode. Working electrode (WE) was a CS embedded in PVC holder using epoxy resin and the uncovered area of the electrode toward solution is 0.34 cm^2. Firstly, WE was immersed in a test solution at an open circuit potential (OCP) for 30 min, until a steady state was reached. PP and EIS measurements were carried out at OCP in the potential range from -800 to -300 mV

vs. SCE with a scan rate 0.2 mV s^{-1} and in the frequency range of 100 kHz–30 mHz at a small alternating voltage perturbation (10 mV) at 20 °C, respectively.

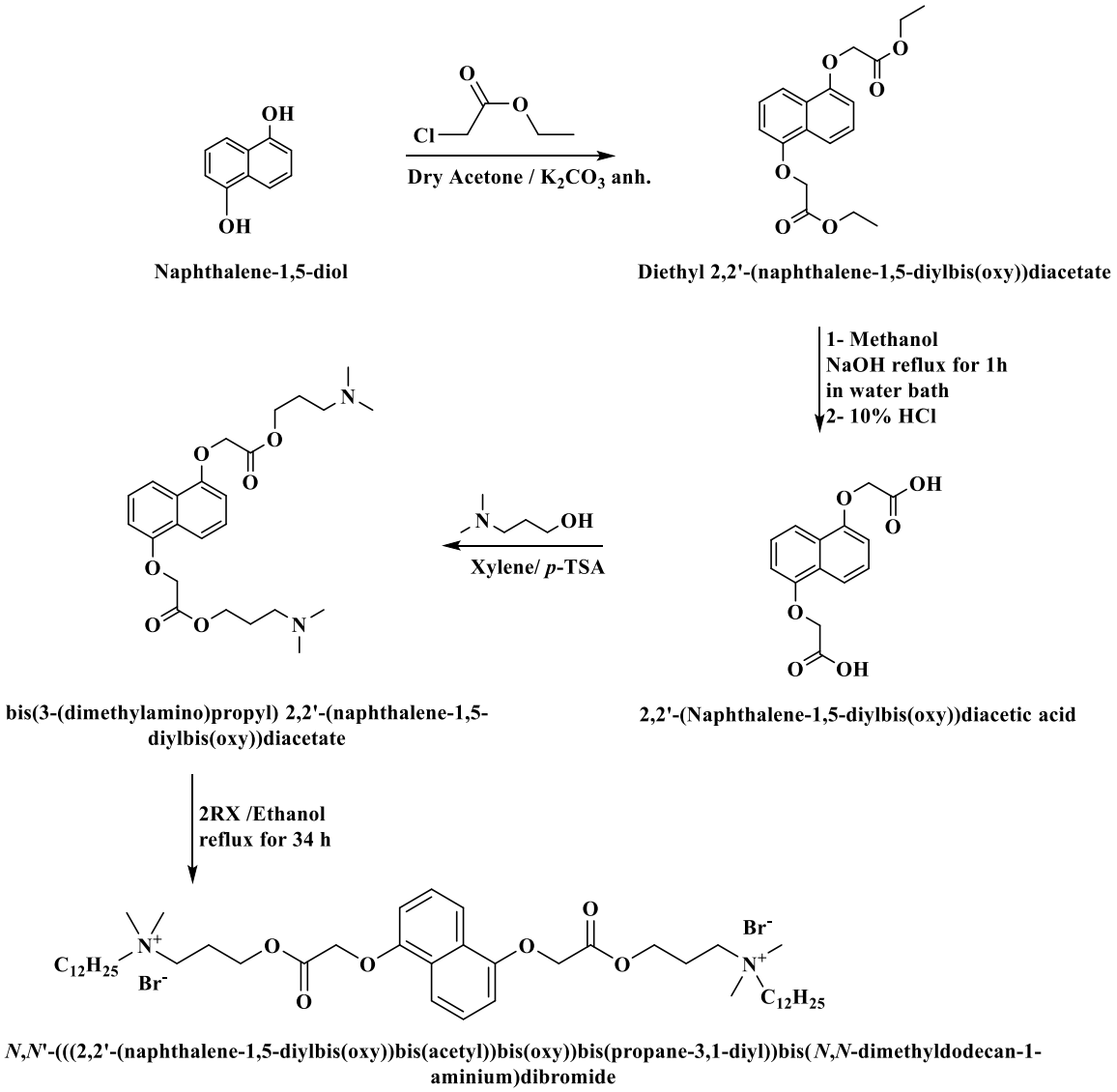

Fig. 1: The scheme of the novel synthesized cationic gemini surfactant (NCGSN).

2.6 Scanning electron microscopy (SEM) and Energy dispersive X-ray analyzer (EDX)

SEM & EDX results of CS surface were listed after immersion of CS coupons in 5% HCl in the absence and presence of NCGSN using SEM Model Quanta 250 FEG (Field Emission Gun).

3. Results and discussion

3.1. Structure confirmation

The chemical structure of Diethyl 2,2'-(naphthalene-1,5-diylbis(oxy))diacetate confirmed by:

FT-IR (KBr cm^{-1}): 3061.028 (Ar-H), 2928.610, 2909.576 (aliph. C-H) and at 1755.489 (C=O).

The mass spectrum (**Fig. 2**) showed that a molecular ion peak and base peak m/z 332 (100%).

The chemical structure of 2,2'-(Naphthalene-1,5-diylbis(oxy))diacetic acid confirmed by:

FT-IR (KBr cm^{-1}): 3059.44 (Ar-H), 2909.7, 2787.179 (aliph. C-H) and at 1742.5, 1707.1 (C=O).

The mass spectrum (**Fig. 3**) showed that a molecular ion peak m/z 276 (40.4%) together with other peaks at m/z (%) 218, $C_{12}H_{10}O_4$, (56), 159, $C_{12}H_7O_2$, (55.69) and 130.84 (100).

The chemical structure of bis(3-(dimethylamino)propyl) 2,2'-(naphthalene-1,5-diylbis(oxy))diacetate confirmed by:

FT-IR (KBr cm^{-1}): 3061.918 (Ar-H), 2970.251, 2945.868, 2861.234 and 2817.580 (aliph. C-H) and at 1762.016 (C=O).

The mass spectrum (**Fig. 4**) showed that a molecular mass m/z (%); 446 (3.54) together with other peaks at $C_{20}H_{30}O_4N_2$, 362(100%), 57.88 (64.52).

^{1}HNMR (DMSO-d6) spectrum (**Fig. 5**), 400 MHz; δ, ppm at: (7.8305, 7.8095) and (7.7799, 7.7589)(2H m, Ar-H), (7.4297, 7.4097, 7.3897) and (7.3636, 7.3436, 7.3236) (2H, t, *J*= 8Hz Ar-H), (6.9570, 6.9377) and (6.8301, 6.8109) (2H, 2d, *J*1= 7.72, *J*2= 7.68 Hz, Ar-H), 4.6161(4H, s, 2 O-C**H**$_2$-COO), 4.1999, 4.1841,4.1683) (4H, t, *J*=6.32 Hz, 2 -COOC**H**$_2$-CH_2), (3.4524, 3.4370, 3.4216) (4H, t, *J*= 6.16 Hz, 2-C**H**$_2$N), (2.3734-2.1952)(12H, s, 2-CH_2CH_2NC**H**$_3)_2$), 1.7582-1.7195) (4H, m, 2-C**H**$_2CH_2N(CH_3)_2$.

The chemical structure of *N,N'*-(((2,2'-(naphthalene-1,5-diylbis(oxy))bis(acetyl))bis(oxy)) bis(propane-3,1-diyl))bis(*N,N*-dimethyldodecan-1-aminium)dibromide confirmed by:

FT-IR (KBr cm^{-1}): (Ar-H), 2925.331, 2855.258 (aliph. C-H) and at 1756.894 (C=O).

The mass spectrum (**Fig. 6**) showed that a molecular mass m/z (%); 942, (6.65) together with a base peak at 472 (100%).

^{1}HNMR spectrum (**Fig. 7**) (DMSO) 400 MHz; δ(ppm) at: (0.8740, 0.8631 and 0.8522) (6H, t, *J*=4.36Hz, 2C**H**$_3(CH_2)_{11}$, (1.2195 - 1.2549) (m, 40H, $2CH_3(C$**H**$_2)_{10}CH_2$), (1.6993–1.7376) (4H, m, 2C**H**$_2CH_2N$), 3.0060(12H, s, 2-$CH_2CH_2N^+(C$**H**$_3)_2$), 3.4483, 3.4636 and 3.4789(8H, t, *J*= 6.12 Hz, 2C**H**$_2N^+C$**H**$_2$), 4.1841, 4.2018, 4.2196 and 4.2373 (4H, 2d, *J*=7.08 2COOC**H**$_2$-CH_2), 4.4810 (4H, s, -O-C**H**$_2$-COO), (6.9349-6.9541) (2H, d, *J*=7.68 Hz, Ar-H), (7.3949, 7,4149 and 7.4349)(2H, t, *J*=8 Hz, Ar-H), [(7.8304-7.8093)(2H, d, *J*=8.44 Hz, Ar-H)].

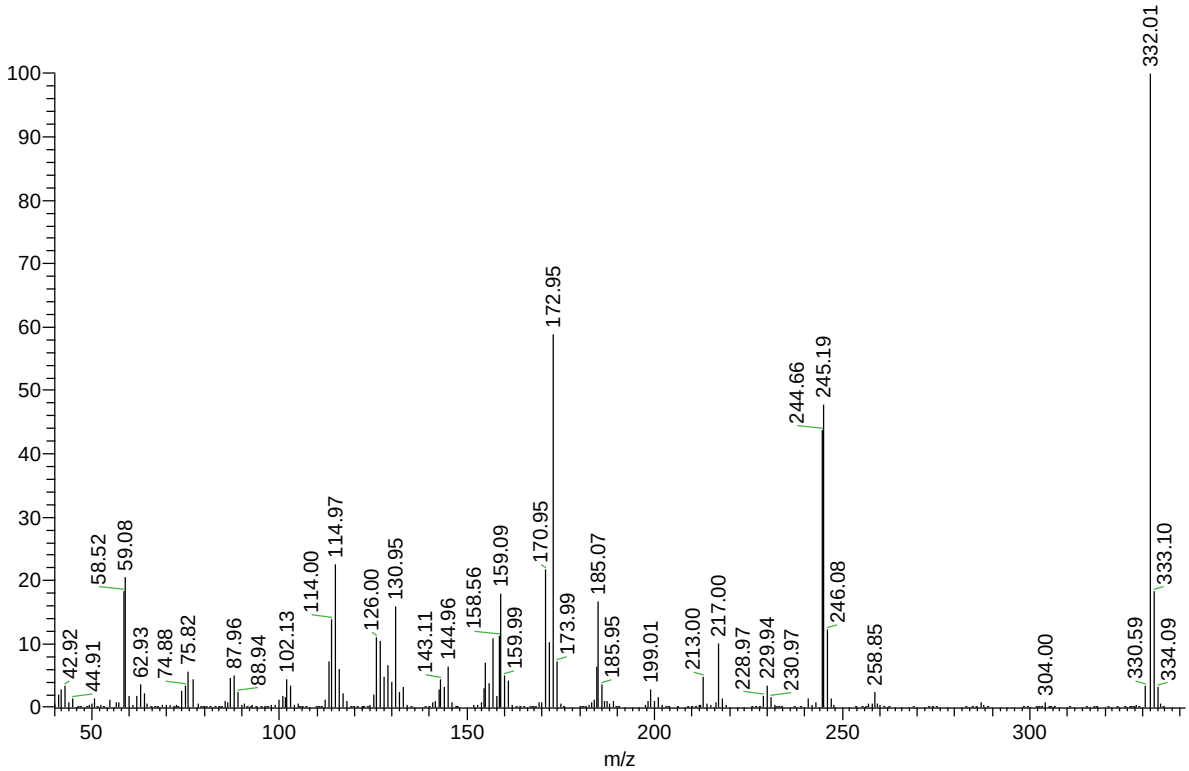

Fig. 2: Mass spectrum of Diethyl 2,2'-(naphthalene-1,5-diylbis(oxy))diacetate.

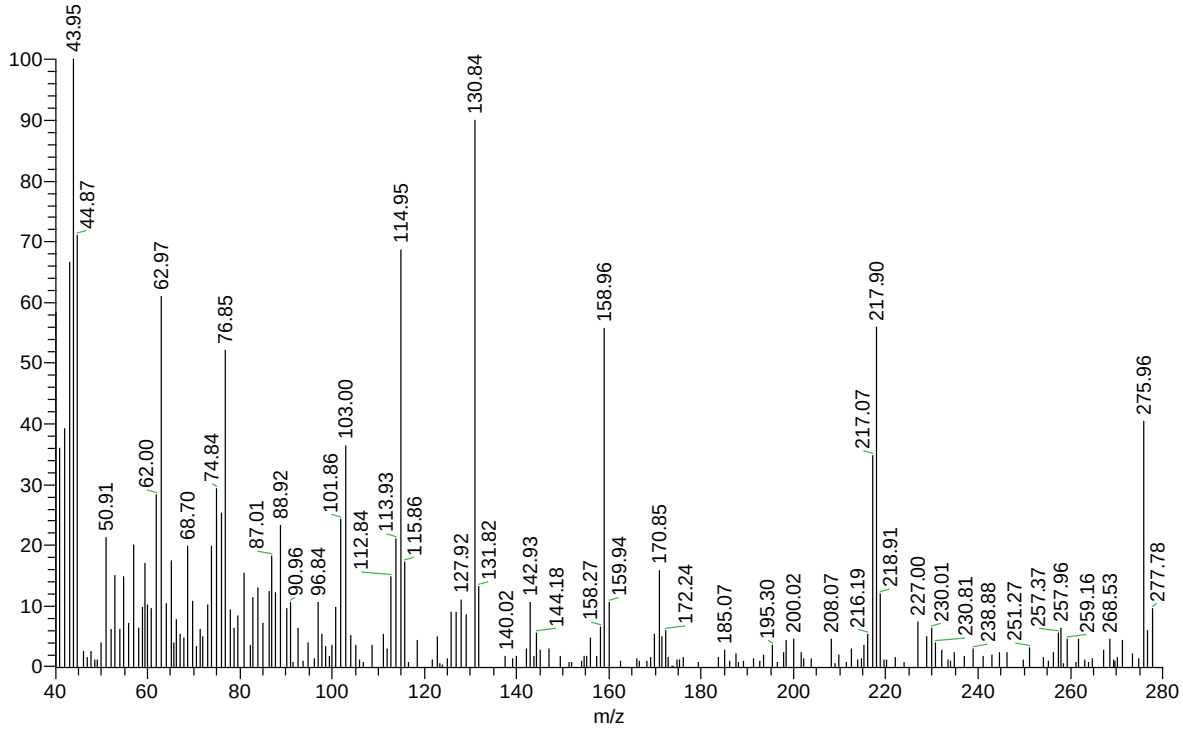

Fig. 3: Mass spectrum of 2,2'-(Naphthalene-1,5-diylbis(oxy))diacetic acid.

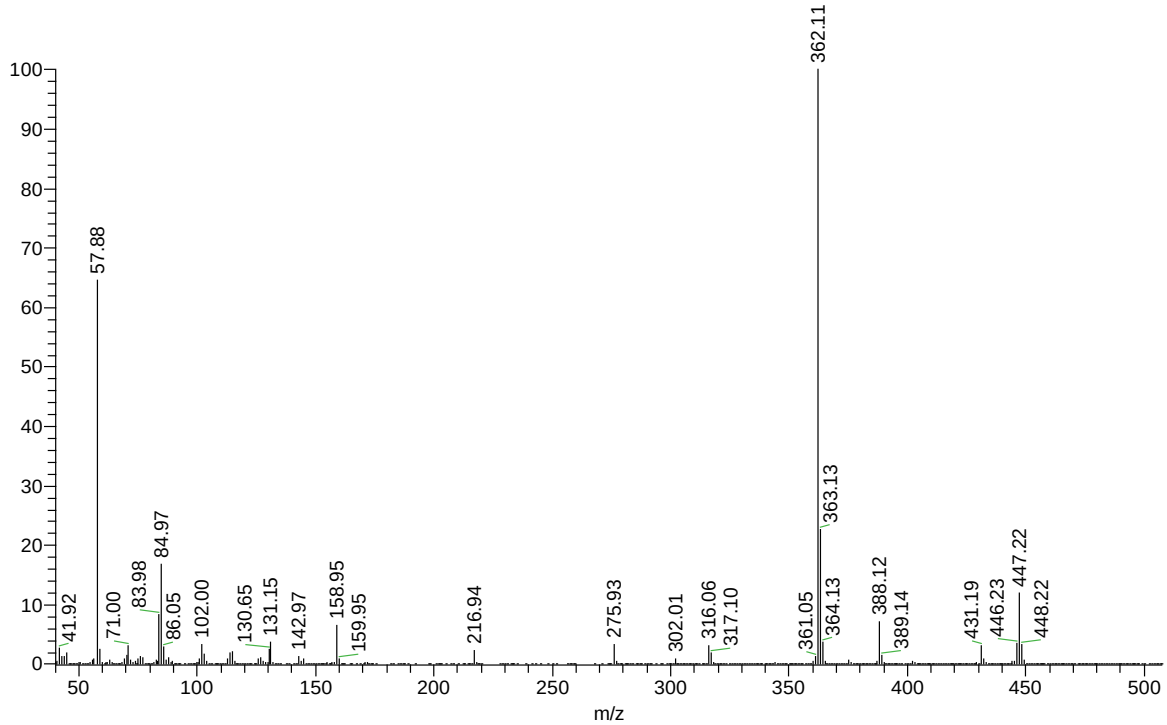

Fig. 4: Mass spectrum of bis(3-(dimethylamino)propyl) 2,2'-(naphthalene-1,5-diylbis(oxy))diacetate.

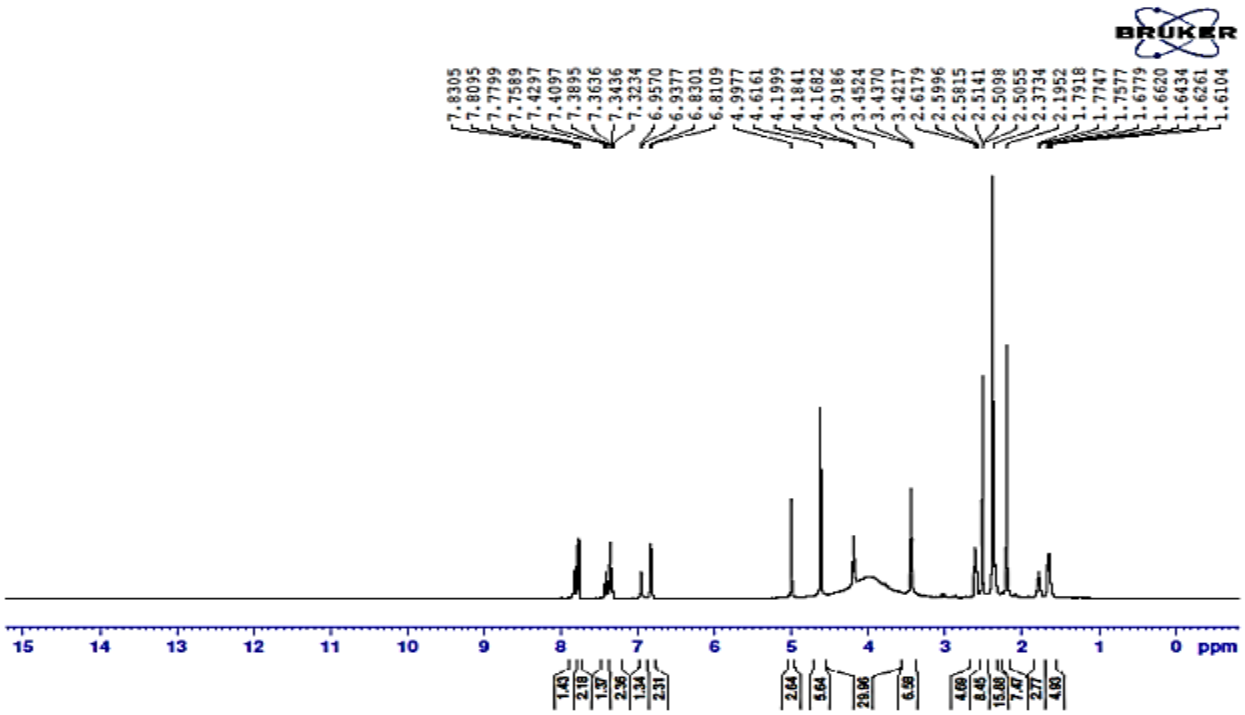

Fig. 5: ^{1}HNMR spectrum of bis(3-(dimethylamino)propyl) 2,2'-(naphthalene-1,5-diylbis(oxy))diacetate.

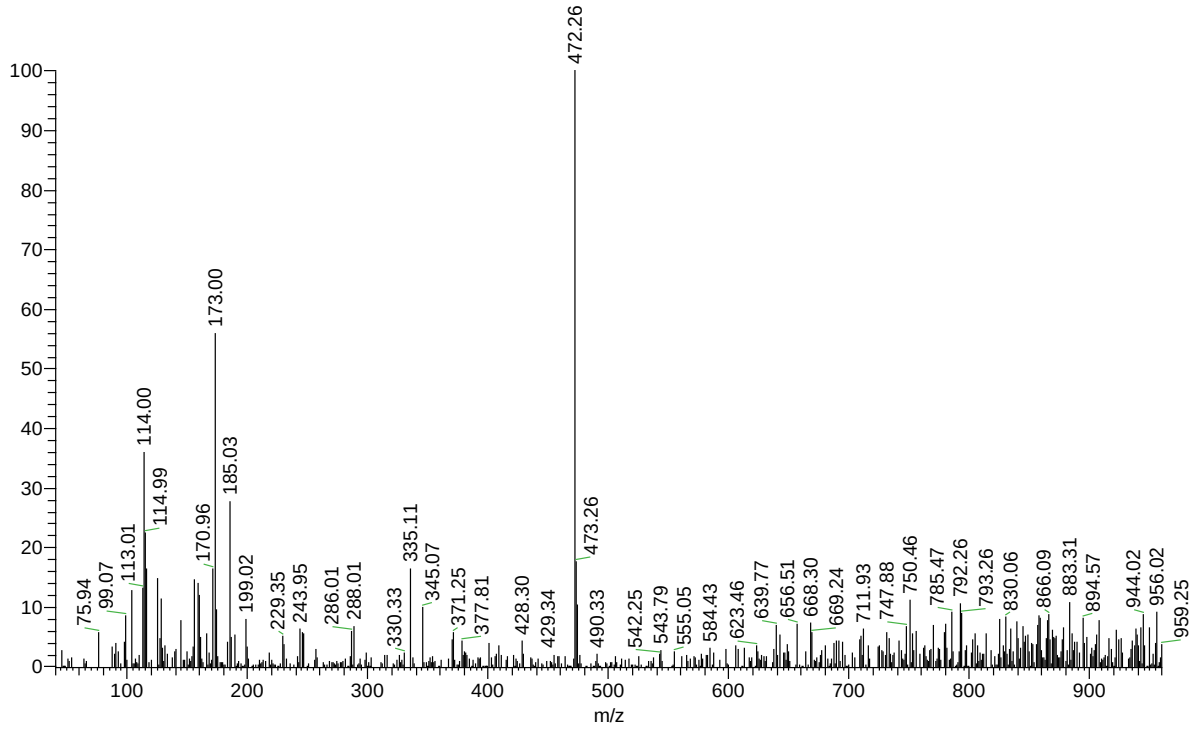

Fig. 6: Mass spectrum of *N*,*N'*-(((2,2'-(naphthalene-1,5-diylbis(oxy))bis(acetyl))bis(oxy))bis(propane-3,1-diyl)) bis(*N*,*N*-dimethyldodecan-1-aminium)dibromide.

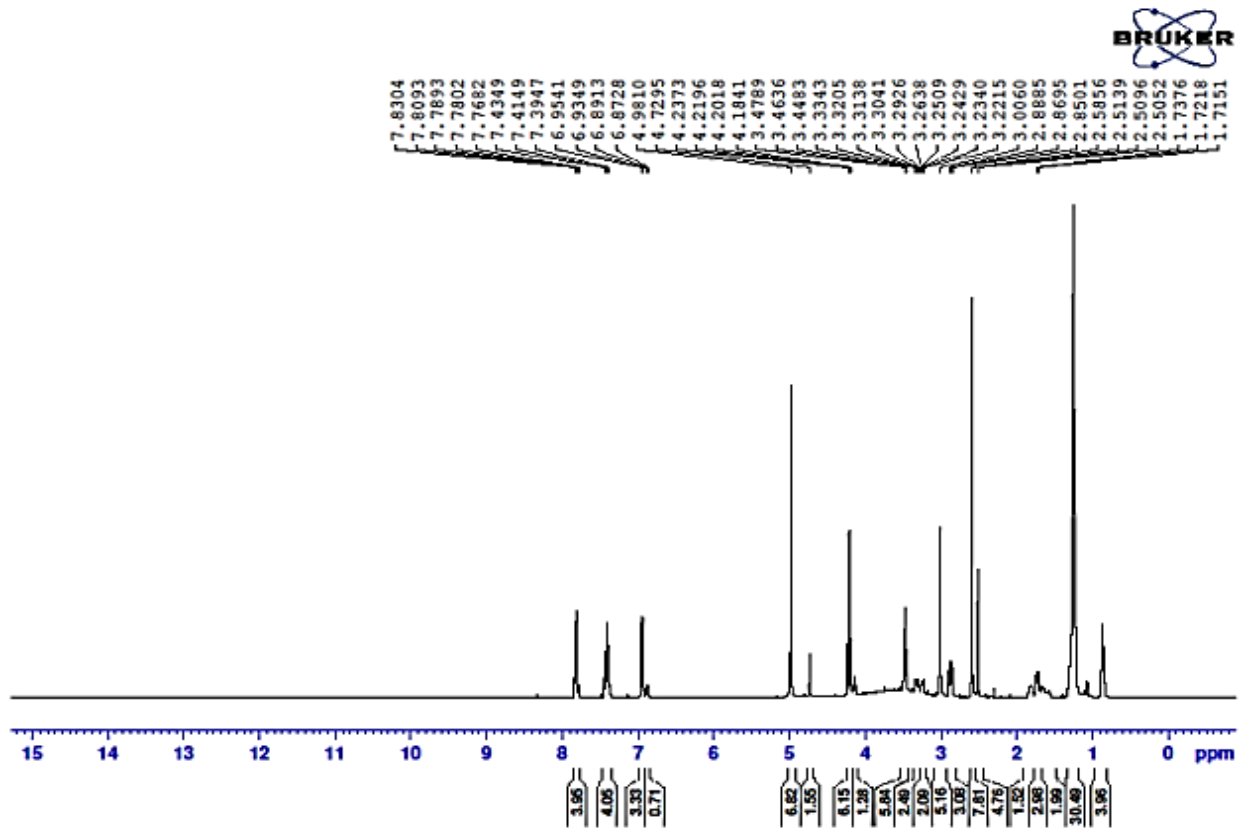

Fig. 7: ^{1}HNMR spectrum of *N,N'*-(((2,2'-(naphthalene-1,5-diylbis(oxy))bis(acetyl))bis(oxy))bis(propane-3,1-diyl)) bis(*N,N*-dimethyldodecan-1-aminium)dibromide.

3.2. Surface active properties

Critical micelle concentration (C_{cmc}) and effectiveness (π_{cmc})

The critical micelle concentration (C_{cmc}) of NCGSN was determined through plotting the surface tension (γ) versus -log C as denoted in **Fig. 8.** C_{cmc} value of NCGSN was determined from the break point plots. NCGSN has good effect of reducing the surface tension and that refers to the effectiveness (π_{cmc}) at C_{cmc}, which was calculated from the next Eq. **[11,12]:**

$$\pi_{cmc} = \gamma_o - \gamma_{cmc} \qquad (1)$$

where, γ_o & γ_{cmc} are the surface tension of pure water and at C_{cmc} at given temperature.

The values of γ_{cmc} and π_{cmc} for NCGSN are given in **Table 1.**

Surface excess (Γ_{max}) & minimum surface area (A_{min})

Γ_{max} & A_{min} are the concentration and the minimum area of NCGSN at the air/solution interface where the surfactant concentration is always higher at the interface than that in the bulk solution.

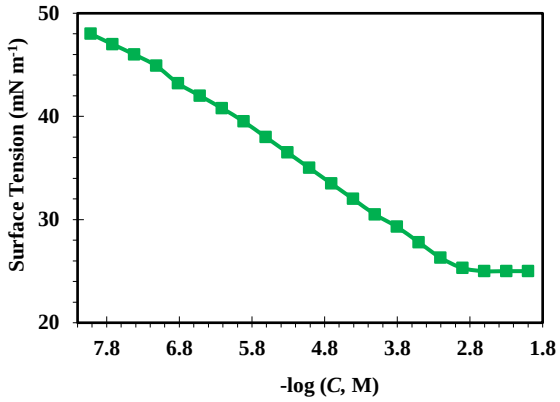

Fig. 8: Variation of the surface tension with concentration of NCGSN in double distilled water at 25 °C.

Table 1: Surface tension parameters of NCGSN in double distilled water at 25 ºC

C_{cmc} (M)	γ_{cmc} (mN m^{-1})	π_{cmc} (mN m^{-1})	$\Gamma_{max} \times 10^{11}$ (mol cm^{-2})	A_{min} (nm^2)
0.0012	25.3	46.7	9.93	1.67

Γ_{max} & A_{min} were calculated by the Gibbs's adsorption through plotting γ against ln C where the slope refers to d γ /d ln C **[13,14]:**

$$\Gamma_{max} = \left(\frac{-1}{nRT}\right)\left(\frac{d\gamma}{d\ln C}\right) \quad (2)$$

$$A_{min} = \frac{10^{14}}{N_A \Gamma_{max}} \quad (3)$$

Γ_{max} & A_{min} values were calculated and represented in **Table 1**. These obtained results exhibited that NCGSN regards a good surface agent.

3.3. Weight loss results

The corrosion rate (k) and inhibition efficiency (η_w) were calculated using the following equations **[15-17]**:

$$k = \frac{\Delta W}{At} \quad (4)$$

$$\eta_w = \frac{(k_{free} - k_{inh})}{k_{free}} \times 100 \quad (5)$$

where ΔW is the average WL, A is the surface area in cm^2, t is the time in hour, k_{free} and k_{inh} are the corrosion rates of CS in 5% HCl in the absence and presence of different concentrations of NCGSN, respectively.

WL data of the corrosion of CS in 5% HCl without and with different concentrations of NCGSN is listed in **Table 2**. WL decreases significantly in the presence of NCGSN compared to 5% HCl solution without NCGSN. It was found that the k depends on the concentration of NCGSN and this indicates that the NCGSN additives inhibit the corrosion of CS in 5% HCl solution and the inhibition efficiency increases with increasing its concentration through forming a protective layer on CS surface. Acid pickling of CS is usually carried out at temperature up to 60°C in different concentrations of HCl. Accordingly; pickling inhibitors are expected to be chemically stable to provide high protective efficiency under the conditions mentioned above **[18]**. Also, we note the η_w values of NCGSN decrease with increasing the temperature **[19]**. The corrosion rate of CS increases slowly with increasing the temperature in the presence of NCGSN. This result confirms that NCGSN acts as an efficient inhibitor in the range of temperature studied.

3.4. Activation energy (E_a) of corrosion process

The values of E_a were calculated from Arrhenius equation **[20]:**

$$k = Ae^{(E_a|RT)} \quad (6)$$

Fig. 9 represents plot of ln corrosion rate (k) versus (1/T) for CS in 5% HCl in the absence and presence of various concentrations of NCGSN. The obtained lines have slope equal to (-E_a/R). Values of E_a were obtained from slope of straight line and represented in **Table 2**. E_a values which were obtained in the presence of NCGSN are greater than those obtained in 5% HCl solution. This indicated that the adsorption of NCGSN on CS surface is mainly physical adsorption than chemical adsorption **[21].**

Table 2
Weight loss and activation energy results for CS in 5% HCl with and without different concentrations of NCGSN at various temperatures

Inhibitor conc. (M)	20 ºC			40 ºC			60 ºC			80 ºC			E_a
	k (mg cm^{-2} h^{-1})	Θ	η_w (%)	k (mg cm^{-2} h^{-1})	Θ	η_w (%)	k (mg cm^{-2} h^{-1})	Θ	η_w (%)	k (mg cm^{-2} h^{-1})	Θ	η_w (%)	
-	0.5665	-	-	1.4453	-	-	3.0789	-	-	5.8352	-	-	33.41
1×10^{-4}	0.0796	0.86	85.95	0.2532	0.82	82.48	0.7547	0.75	75.49	1.7192	0.71	70.54	44.41
5×10^{-4}	0.0359	0.94	93.67	0.1806	0.88	87.51	0.5181	0.83	83.17	1.1933	0.80	79.55	50.04
1×10^{-3}	0.0238	0.96	95.79	0.1164	0.92	91.95	0.3768	0.88	87.76	0.9845	0.83	83.13	53.26
5×10^{-3}	0.0121	0.98	97.87	0.0699	0.95	95.16	0.2146	0.93	93.03	0.6969	0.88	88.06	57.33

3.5. Adsorption thermodynamic parameters

The adsorption of the NCGSN molecules on the CS surface in aqueous solutions regards substitution process between the NCGSN molecules and water molecules adsorbed on CS surface.

The inhibition mechanism of NCGSN illustrates by adsorption isotherm. The surface coverage (θ) at a certain temperature was calculated from the next equation **[22-24]**:

$$\theta = \frac{(W_{free} - W_{inh})}{W_{free}} \quad (7)$$

where W_{free} and W_{inh} are the WL of CS due to the dissolution in 5% HCl in the absence and presence of different concentrations of NCGSN, respectively.

Langmiur adsorption isotherm for CS in 5% HCl plotted as C/θ against C as shown in **Fig. 10**. A straight line is obtained with a slope close to unity and intercept equal ($1/K_{ads}$). The obtained data fitted to the Langmiur adsorption isotherm which characterized by the next equation **[25-27]**:

$$\frac{C}{\theta} = \frac{1}{K_{\text{ads}}} + C \qquad (8)$$

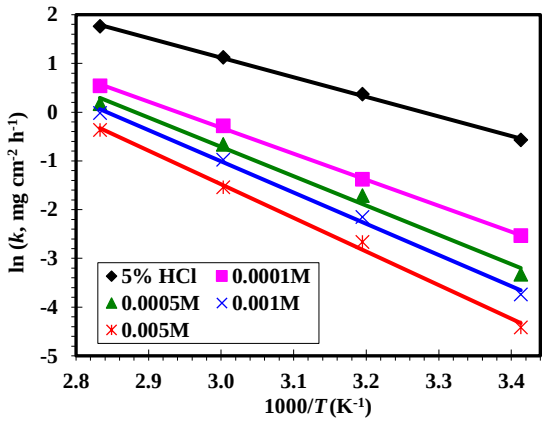

Fig. 9: ln k versus $1/T$ curves for CS dissolution in the absence and presence of different concentrations of NCGSN in 5% HCl solution.

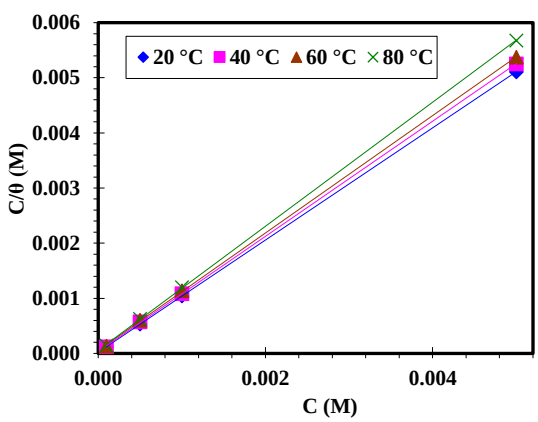

Fig. 10: Langmuir isotherm adsorption model of NCGSN on CS surface in 5% HCl at different temperatures.

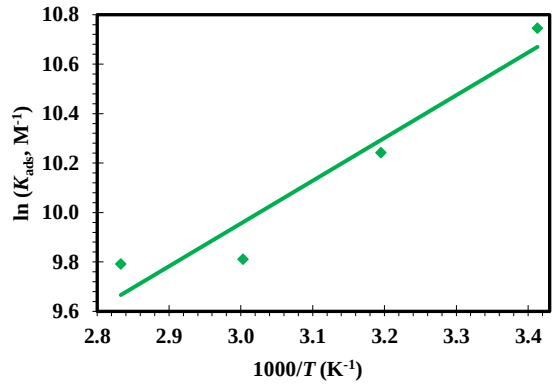

Fig. 11: The relationship between ln K_{ads} and $1/T$ for CS in 5% HCl solution containing different concentrations of NCGSN.

The adsorption free energy ($\Delta G°_{ads}$), adsorption heat ($\Delta H°_{ads}$) and adsorption entropy ($\Delta S°_{ads}$) can be calculated by mathematical method depending on various temperatures.

$\Delta G°_{ads}$ values are calculated through adsorption equilibrium constant (K_{ads}) as the next equation **[28,29]**:

$$\Delta G°_{\text{ads}} = -RTln(55.5K_{\text{ads}}) \qquad (9)$$

$\Delta G°_{ads}$ characterize the interaction between the adsorbed molecules and metal surface **[30]**. When values of $\Delta G°_{ads}$ up to -20 kJ mol^{-1}, they are consistent with the electrostatic attraction between NCGSN molecules and CS (physical adsorption) while those more negative than -40 kJ mol^{-1} involve sharing or transfer of electrons from the NCGSN molecules to CS surface to form a coordinate bond (chemisorption) **[31]**. In the present study, the values of $\Delta G°_{ads}$ are ranging between -35.96 and -40.52 kJ mol^{-1}. This indicated that the adsorption of NCGSN onto the CS surface is physical-chemical adsorption **[32].** Results represented in **Table 3** showed that $\Delta G°_{ads}$ values decreases with increasing the temperature indicating the adsorption of NCGSN is more spontaneous with increasing temperature.

$\Delta H°_{ads}$ was calculated agreeing to the Van't Hoff equation **[33,34]:**

$$\ln K_{\text{ads}} = \left(\frac{\Delta H^{o}_{\text{ads}}}{RT}\right) + \text{constant} \qquad (10)$$

We can get $-\Delta H°_{ads}$ from slope of obtained straight line of plotting ln (K_{ads}) vs $1/T$ according to Eq. (10) as represented in **Fig. 11**. Negative sign of $\Delta H°_{ads}$ value in **Table 3** indicated that the adsorption process of NCGSN was exothermic **[35].** The value of $\Delta H°_{ads}$ which is -14.38 indicated that the NCGSN adsorption on CS surface in 5% HCl solution proceeds by

physical more than chemical adsorption for the NCGSN molecules on the CS surface.

ΔS^{o}_{ads} was obtained using the basic thermodynamic equation [36]:

$$\Delta G^{o}_{ads} = \Delta H^{o}_{ads} - T\Delta S^{o}_{ads} \quad (11)$$

The positive values of ΔS^{o}_{ads} indicated the spontaneous adsorptive ability of the NCGSN species on CS surface [37].

Table 3: Standard thermodynamic adsorption parameters in the presence of different concentrations of NCGSN on CS in 5% HCl at different temperatures

Temp. (°C)	K_{ads} (M^{-1})	ΔG^{o}_{ads} (kJ mol^{-1})	ΔH^{o}_{ads} (kJ mol^{-1})	ΔS^{o}_{ads} (J mol^{-1} K^{-1})
20	46407	-35.96	-14.38	73.65
40	28054	-37.10		72.60
60	18238	-38.28		71.78
80	17871	-40.52		74.05

3.6. Potentiodynamic polarization results

Typical current-potential of NCGSN in 5% HCl in the absence and presence of different concentrations of NCGSN are shown in Fig. 12. Values of Tafel parameters such as corrosion potential (E_{corr}), anodic & cathodic Tafel slopes (β_a & β_c, respectively) and corrosion current density (i_{corr}) are listed in Table 4. The inhibition efficiency (η_p) was calculated from polarization measurements according to the next relation [38]:

$$\eta_p = \frac{i_{corr} - i_{corr}(inh)}{i_{corr}} x\ 100 \quad (12)$$

where i_{corr} and i_{corr}(inh) are the corrosion current densities for CS in the uninhibited and inhibited solutions, respectively.

The presence of NCGSN does not unusually shift the E_{corr} and the values of β_a and β_c change slightly in the range less than 85 mV. This suggests that the corrosion mechanism of CS in 5% HCl solution does not change when the NCGSN is added. It is indicating that NCGSN is a mixed type because they prevent both the anodic and cathodic processes. Where NCGSN adsorb first onto CS surface and subsequently lead to reduction of surface area available for corrosion reactions by blocking merely the reaction sites of CS surface [39]. It was found that i_{corr} decreases with increasing the NCGSN concentration, which indicates that the presence of NCGSN retards the dissolution of CS in 5% HCl and the inhibition value depends on its concentration.

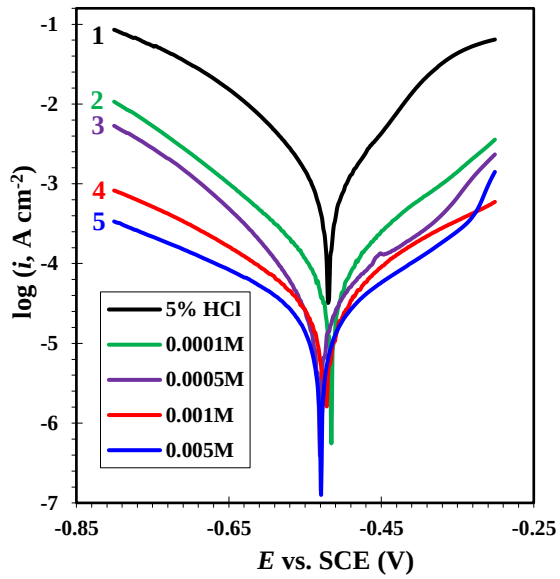

Fig. 12: Anodic and cathodic polarization curves for CS at 20 °C in 5% HCl with and without different concentrations of NCGSN.

Table 4
Potentiodynamic polarization parameters for CS in 5% HCl with and without different concentrations of NCGSN at 20 °C

Conc. of inhibitor (M)	E_{corr} (mV)	i_{corr} (mA cm^{-2})	β_a (mV dec^{-1})	β_c (mV dec^{-1})	η_p (%)
0.00	-511.8	0.6133	81.3	-90.6	-
$1x10^{-4}$	-518.0	0.0942	141.8	-130.0	84.64
$5x10^{-4}$	-532.2	0.0478	174.9	-118.2	92.21
$1x10^{-3}$	-525.8	0.0323	164.2	-180.9	94.73
$5x10^{-3}$	-531.8	0.0185	160.3	-191.7	96.98

3.7. EIS results

The semicircular capacitive loops of CS in 5% HCl solution in the absence and presence of different concentrations of NCGSN are noted as shown in Fig. 13. This figure shows that the addition of NCGSN results in an increase in both real and imaginary impedance. This is due to the formation of an isolating layer of NCGSN on CS surface. The increment in charge transfer resistance (R_{ct}) with the increment in the concentration of NCGSN is due to the increase in surface coverage for active sites on CS surface. Fig. 13 shows the frequency dispersion in Nyquist plot at low frequency and this behavior results to irregularities and heterogeneities of CS surface [40].

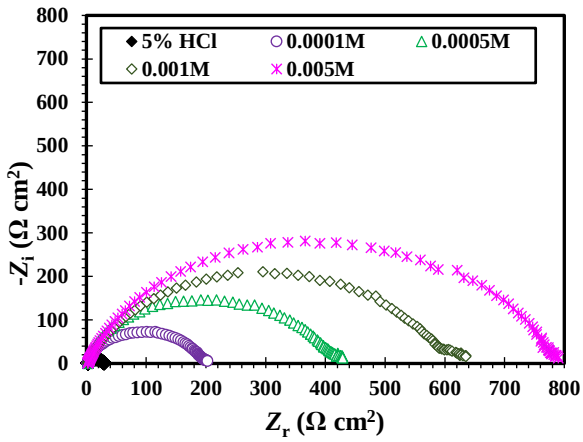

Fig. 13: Nyquist plots for CS at 20 °C in 5% HCl with and without different concentrations of NCGSN.

The inhibition efficiency got from the charge-transfer resistance is calculated using the next equation **[41]**:

$$\eta_I = \frac{R^\circ_{ct} - R_{ct}}{R^\circ_{ct}} x100 \qquad (13)$$

where R^o_{ct} and R_{ct} are the charge-transfer resistance values with and without inhibitor, respectively.

Fig. 13 shows that the impedance (Z_{CPE}) value increases with increasing the NCGSN concentration. CPE impedance is calculated by **[42,43]**:

$$Z_{CPE} = Q^{-1} (i\omega_{max})^{-n} \qquad (14)$$

where Q, $\omega_{max} = 2\pi f_{max}$, f, i, n are constant phase element, the angular frequency, the frequency at the maximum imaginary element of the impedance, the imaginary number and a coefficient of surface inhomogeneity, respectively.

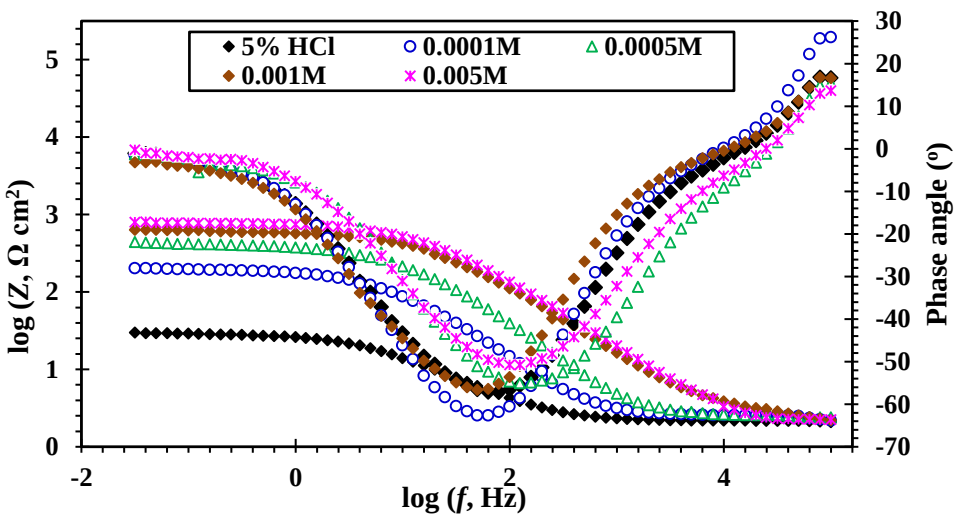

Fig. 14: Bode and phase plots for CS at 20 °C in 5% HCl with and without different concentrations of NCGSN.

Fig. 14 detects only one maximum curvature in Bode plot. This means the equivalent circuit to this system formed one circuit only. This circuit (**Fig. 15**) consists of solution resistance (R_s) and CPE as a substitute to capacitance of double layer (C_{dl}) and non-ideal capacitance in parallel with R_{ct} as used in previous CS/acid interface model **[44,45]**.

The values of C_{dl} calculated using the next equation **[46,47]**:

$$C_{dl} = Q(\omega_{max})^{n-1} \qquad (15)$$

The results obtained from this complex plot are given in **Table 5**.

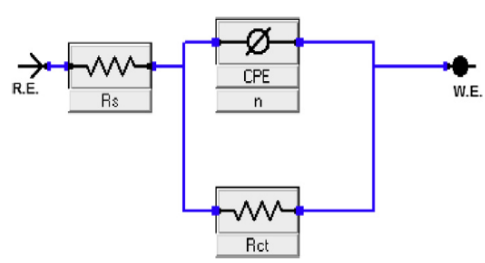

Fig. 15: The corresponding equivalent circuits used to fit the EIS experimental data for CS in 5% HCl with and without different concentrations of NCGSN.

Table 5: Electrochemical impedance parameters for CS in 5% HCl with and without different concentrations of NCGSN at 20 °C

Conc. of inhibitor (M)	R_s (Ω cm^2)	Q_{dl} (mΩ^{-1}s^n cm^{-2})	n	R_{ct} (Ω cm^2)	*Chsq*	C_{dl} (μF cm^{-2})	η_I (%)

0.00	2.1	0.7845	0.80	29.92	0.00082	116.5	-
$1x10^{-4}$	2.7	0.1151	0.90	187.6	0.00386	18.6	84.05
$5x10^{-4}$	2.5	0.0674	0.91	392.4	0.00514	8.8	92.38
$1x10^{-3}$	2.9	0.0323	0.85	583.1	0.00837	6.4	94.87
$5x10^{-3}$	2.0	0.0263	0.86	752.8	0.00743	5.1	96.03

From **Table 5**, it is apparent that R_{ct} value of CS in uninhibited solution increases significantly after the addition of NCGSN. The values of *n* were in the range from 0.80 to 0.91, representative non-ideal capacitive actions.

From **Table 5**, the addition of NCGSN to the corrosive solution decreases the double layer capacitance. The double layer between the charged metal surface and the solution is considered as an electrical capacitor. The decrease in this capacity could be assigned to the regular replacement of water molecules by the adsorption of NCGSN at the CS/solution interface. The adsorption process is due to surface film formation of NCGSN protecting the metal against corrosion **[48-51]**. EIS results revealed that corrosion inhibition efficiency of the NCGSN increases with increasing its concentration.

3.8. SEM

Fig. 16a,b shows SEM image of CS coupon in 5% HCl in the absence and presence of 0.005M NCGSN for 24 h at 20 ºC. **Fig. 16a** reveals that CS surface was strongly damaged in absence of NCGSN while **Fig. 16b** reveals that CS surface is protected by formed protective film of NCGSN. This image confirms the high inhibition efficiency of NCGSN.

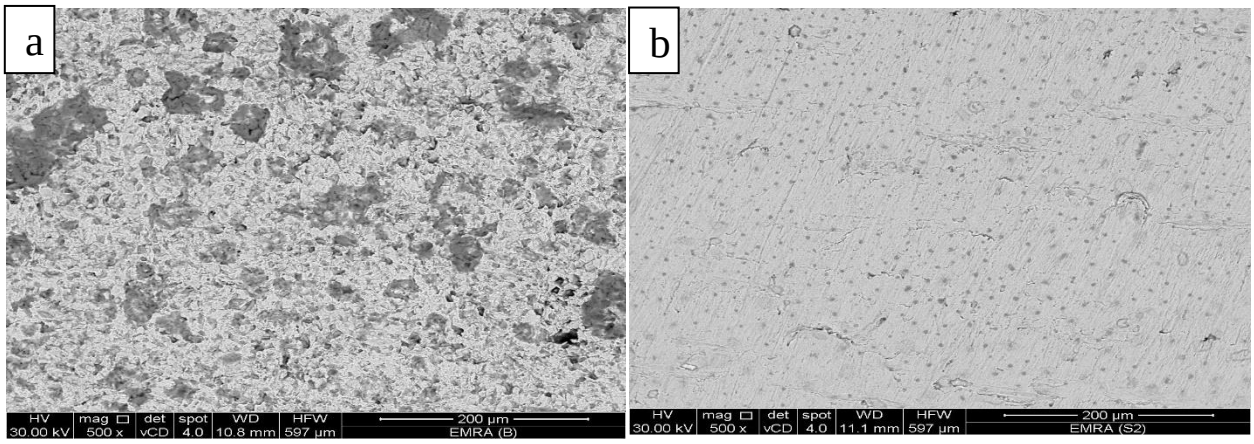

Fig. 16: SEM images of CS in 5% HCl solution at 20 °C: (a) in the absence of the inhibitor and (b) in the presence of NCGSN at 5×10^{-3} M.

3.9. EDX

Fig. 17a,b shows EDX micrographs of carbon steel sample in 5% HCl in the absence and presence 5 x 10^{-3} M of the NCGSN, respectively, at 20 ºC after 24 h immersion. It is clear that the micrograph detected the presence of oxygen and chlorine elements (corrosive elements) for the sample immersed in 5% HCl solution and absence of the corrosive elements and exhibits C, O and N atoms of NCGSN molecules for the sample immersed in the inhibited solution. Such results are due to adsorption of protective barrier films of the inhibitor species on the metal surface which reduce the corrosion rate. These results are matched with those obtained from SEM micrographs.

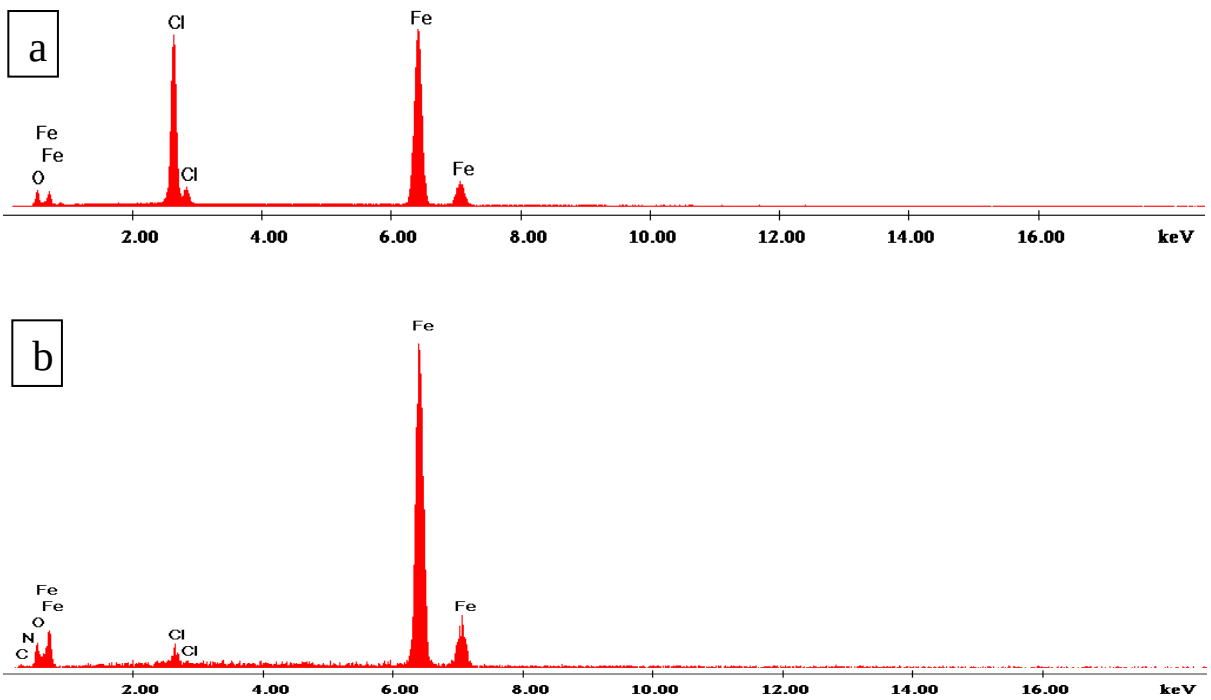

Fig. 17: EDX chart of CS in 5% HCl solution at 20 °C: (a) in the absence of the inhibitor and (b) in the presence of NCGSN at 5×10^{-3} M.

3.10. Inhibition mechanism

Adsorption of NCGSN on CS surface may occur through one or more of the following ways: (a) physical contact between NCGSN and CS surface through the static charges on molecules and metal, (b) chemical interaction of electron pairs in NCGSN with CS, (c) interaction of double bond electrons with CS and/or, (d) blend of two or more of previous types (a–c). The adsorption of quaternary ammonium salt on CS surface in HCl medium begins with ammonium ion (N^+) then followed by counter ion (Br^{-1}) because CS surface becomes negatively charged in HCl **[52]**. The NCGSN molecules are adsorbed on charged sites of CS surface through electrostatic attraction force between the ammonium groups (N^+) and bromide ions with anodic-cathodic locations on CS surface but π electron of benzene ring and lone pair of electron of O atoms formed chemical bond with vacant d orbital of iron.

4. Conclusion

1. The synthesized novel NCGSN is a good corrosion inhibitor for CS during pickling process. The inhibitory efficiency of NCGSN depends on its concentration.
2. Surface tension results exhibited that NCGSN regards a good surface agent.
3. NCGSN acts as mixed-type inhibitor.
4. The high inhibition efficiency of NCGSN was explained by adsorption of NCGSN molecules on CS and formed a protective film.
5. The adsorption of NCGSN on CS surface from 5% HCl solution follows Langmuir adsorption isotherm. The thermodynamic parameters suggest that NCGSN is strongly adsorbed on CS surface.
6. The adsorption of NCGSN on CS surface takes place through electrostatic interactions in addition to charge sharing or transfer from the NCGSN molecules to CS surface to form chemical bonds.
7. SEM & EDX image of CS in 5% HCl in the absence and presence of 0.005 M NCGSN confirmed the WL, PP and EIS results.

Funding: This research received no external funding.

Conflicts of Interest: The authors declare no conflict of interest.

References

[1] Finšgar M., Jackson J., Application of corrosion inhibitors for steels in acidic media for the oil and gas industry: A review, Corros. Sci. 86, 17-41 (2014).

[2] Abdallah M., Hegazy M.A., AlfakeerM., Ahmed H., Adsorption and inhibition performance of the novel cationic gemini surfactant as a safe corrosion inhibitor for carbon steel in hydrochloric acid, Green Chemistry Letters and Reviews 11, 457–468 (2018).

[3] Mahdavian M., Tehrani-Bagha A.R., Alibakhshi E., Ashhari S., Ektefa F., Corrosion of mild steel in hydrochloric acid solution in the presence of two cationic gemini surfactants with and without hydroxyl substituted spacers, Corros. Sci. 137, 62-75 (2018).

[4] Hegazy M.A., El-Tabei A.S., Bedair A.H., Sadeq M.A., Synthesis and inhibitive performance of novel cationic and gemini surfactants on carbon steel corrosion in 0.5 M H_2SO_4 solution, RSC Adv. 5, 64633–64650 (2015).

[5] Abd El-Lateef H.M., Abo-Riya M.A., Tantawy A.H., Empirical and quantum chemical studies on the corrosion inhibition performance of some novel synthesized cationic gemini surfactants on carbon steel pipelines in acid pickling processes, Corros. Sci. 108, 94-110 (2016).

[6] Eagleson, Mary (1994). Concise encyclopedia chemistry (revised ed.). Walter de Gruyter. p. 834. ISBN 978-3-11-011451-5.

[7] ASM handbook. ASM International. Handbook Committee. (10th ed.). Materials Park, Ohio. ISBN 9780871703842. OCLC 21034891.

[8] American Electroplaters and Surface Finishers Society (2002). Proceedings AESF SUR/FIN 2002: Annual International Technical Conference June 24-27, 2002, Chicago, IL. Orlando, FL: American Electroplaters and Surface Finishers Society.

[9] Liu, David; Lipták, Béla G. (1997). Environmental engineers' handbook. CRC Press. p. 973. ISBN 978-0-8493-9971-8.

[10] Fisch, Arline M. (2003). Textile Techniques in Metal: For Jewelers, Textile Artists & Sculptors. Lark Books. p. 32. ISBN 978-1-57990-514-9.

[11] Labena A., Hegazy M.A., Horn H., Müller E., Sulfidogenic-corrosion inhibitory effect of cationic monomeric and gemini surfactants: planktonic and sessile diversity, RSC Adv. 6, 42263–42278 (2016).

[12] Patial P., Shaheen A., Ahmad I., Gemini pyridinium surfactants: synthesis and their surface active properties, J. Surfact. Deterg. 17, 929–935 (2014).

[13] Labena A., Hegazy M.A., Kamel W.M., Elkelish Amr, Hozzein Wael N., Enhancement of a cationic surfactant by capping nanoparticles: synthesis, characterization and multiple applications, Molecules 25, 2007-2025 (2020).

[14] Hegazy M.A., Abd El-Rehim S.S., Emad A. Badr, Kamel W.M., Ahmed H. Youssif, Mono-, di- and tetra-cationic surfactants as carbon steel corrosion inhibitors, J Surfact Deterg 18, 1033–1042 (2015).

[15] Ruby Aslam, Mohammad Mobin, Jeenat Aslam, Hassane Lgaz, Ill-Min Chung, Inhibitory effect of sodium carboxymethylcellulose and synergistic biodegradable gemini surfactants as effective inhibitors for MS corrosion in 1 M HCl, J. Mater. Res. Tech. 8, 4521-4533 (2019).

[16] Kaczerewska O., Leiva-Garcia R., Akid R., Brycki B., Pospieszny T., Effectiveness of O-bridged cationic gemini surfactants as corrosion inhibitors f or stainless steel in 3M HCl: Experimental and theoretical studies, J Mol. Liq. 249, 1113-1124 (2018).

[17] Abdallah M., Eltass H.M., Hegazy M.A., Ahmed H., Adsorption and inhibition effect of novel cationic surfactant for pipelines carbon steel in acidic solution, Prot. Met. Phys. Chem. Surf. 52, 721-730 (2016).

[18] El-Tabei A.S., Hegazy M.A., Application of the synthesized novel 3,6,9,12,15,18,21-heptaoxatricosane-1,23-diyl bis(4-((4-(dimethylamino)benzylidene)amino)benzoate) as a corrosion inhibitor for carbon steel in acidic media, J. Disp. Sci. and Tech. 35, 1289-1299 (2014).

[19] Azzam E.M.S., Hegazy M.A., Kandil N.G., Badawi A.M. and Sami R.M., The performance of hydrophobic and hydrophilic moieties in synthesized thiol cationic surfactants on corrosion inhibition of carbon steel in HCl, Egypt. J. Petrol. 24, 493–503 (2015).

[20] Solmaz R., Investigation of adsorption and corrosion inhibition of mild steel in hydrochloric acid solution by 5-(4-dimethylaminobenzylidene) rhodanine, Corros. Sci. 79, 169–176 (2014).

[21] Hegazy M.A., Abd El Rehim S.S., Badawi A.M., Ahmed M.Y., Studying the corrosion inhibition of carbon steel in hydrochloric acid solution by 1-dodecyl-methyl-1H-benzo[d][1,2,3]triazole-1-ium bromide, RSC Advances 5, 49070–49079(2015).

[22] Kubo J., Tanaka Y., Page C.L., Page M.M., Application of electrochemical organic corrosion inhibitor injection to a carbonated reinforced concrete railway viaduct, Constr. Build. Mater. 39, 2–8 (2013).

[23] Han P., He Y., Chen C., Yu H., Liu F., Yang H., Ma Y., Y. Zheng, Study on synergistic mechanism of inhibitor mixture based on electron transfer behavior, Sci. Rep. 6, 33252 (2016).

[24] Noor El-Din M.R., Al-Sabagh A.M. , Hegazy M.A., Study of the inhibition efficiency for some novel surfactants on the carbon steel (Type H-11) pipelines in 0.5 M HCl solution by potentiodynamic technique, J. Disp. Sci. Tech. 33, 1444–1451 (2012).

[25] Chidiebere M.A., Oguzie E.E., Liu L., Li Y., Wang F., Ascorbic acid as corrosion inhibitor for Q235 mild steel in acidic environments, J. Ind. Eng. Chem. 26, 182–192 (2015).

[26] Aljourani J., Raeissi K., Golozar M., Benzimidazole and its derivatives as corrosion inhibitors for mild

steel in 1 M HCl solution, Corros. Sci. 51, 1836–1843 (2009).

[27] Hegazy M.A., Samy R.M., Labena A., Wadaan M.A.M., Hozzein W.N., 4,4'-(((1E,5E)-pentane-1,5-diylidene)bis(azanylylidene))bis(1-dodecylpyridin-1-ium) bromide as a novel corrosion inhibitor in an acidic solution (Part I), Mater. Sci. Eng. C 110, 110673 (2020).

[28] Hegazy M.A., El-Etre A.Y., Berry K.M., Novel inhibitors for carbon steel pipelines corrosion during acidizing of oil and gas wells, Journal of Basic and Environmental Sciences 1, 174-189 (2014).

[29] El-Tabei A.S., Hegazy M.A., Synthesis and characterization of a novel nonionic gemini surfactant as corrosion inhibitor for carbon steel in acidic solution, Chem. Eng. Commun. 7, 851-863 (2015).

[30] Badr, E.A. Inhibition effect of prepared cationic surfactant on the corrosion of carbon steel in 1 M HCl. J. Ind. Eng. Chem., 20, 3361–3366 (2014).

[31] Umoren S., Ebens E.O, The synergistic effect of polyacrylamide and iodide ions on the corrosion inhibition of mild steel in H_2SO_4, Mater. Chem. Phys. 106, 387–393 (2007).

[32] Tang L., Li X., Si Y., Mu G., Liu G., The synergistic inhibition between 8-hydroxyquinoline and chloride ion for the corrosion of cold rolled steel in 0.5 M sulfuric acid, Mater. Chem. Phys. 95, 29–38 (2006).

[33] Hegazy M.A., Abd El Rehim S.S., Badawi A.M., Ahmed M.Y., Studying the corrosion inhibition of carbon steel in hydrochloric acid solution by 1-dodecyl-methyl-1H-benzo[d][1,2,3]triazole-1-ium bromide, RSC Adv. 5, 49070 – 49079 (2015).

[34] Hu Z., Meng Y., Ma X., ZhH. u, Li J., Li C., Cao D., Experimental and theoretical studies of benzothiazole derivatives as corrosion inhibitors for carbon steel in 1 M HCl, Corros. Sci. 112, 563–575 (2016).

[35] Bedair M.A., Soliman S.A., Hegazy M.A., Obot I.B., Ahmed A.S., Empirical and theoretical investigations on the corrosion inhibition characteristics of mild steel by three new Schiff base derivatives, J Adhes. Sci. Tech. 33, 1139-1168 (2019).

[36] Refaey S., Taha F., El-Malak A.A., Inhibition of stainless steel pitting corrosion in acidic medium by 2-mercaptobenzoxazole, Appl. Surf. Sci. 236, 175–185 (2004).

[37] Umoren S., Obot I., Ebenso E., Corrosion inhibition of aluminium using exudate gum from Pachylobus edulis in the presence of halide ions in HCl, J. Chem. 5, 355–364 (2008).

[38] Wang Y., Zuo Y., The adsorption and inhibition behavior of two organic inhibitors for carbon steel in simulated concrete pore solution, Corros. Sci. 118, 24–30 (2017).

[39] Han P., Li W., Tian H., Gao X., Ding R., Xiong C., C. Chen, Designing and fabricating of time-depend self-strengthening inhibitor film: synergistic inhibition of sodium dodecyl sulfate and 4-mercaptopyridine for carbon steel, J. Mol. Liq. 268, 425–437 (2018).

[40] Hegazy M.A., Abdallah M., Alfakeer M., Ahmed H., Corrosion inhibition performance of a novel cationic surfactant for protection of carbon steel pipeline in acidic media, International Journal of Electrochemical Science 13, 6824–6842 (2018).

[41] Kadhum A.H., Mohamad A.B., Hammed L.A., Al-Amiery A.A., San N.H., Musa A.Y., Inhibition of mild steel corrosion in hydrochloric acid solution by new coumarin, Mater. 7, 4335–4348 (2014).

[42] Wang X., Yang H., Wang F., A cationic gemini-surfactant as effective inhibitor for mild steel in HCl solutions, Corros. Sci. 52, 1268–1276 (2010).

[43] Ting Zhou, Jing Yuan, Zhiqing Zhang, Xia Xin, Guiying Xu, The comparison of imidazolium Gemini surfactant [C14-4-C14im]Br2 and its corresponding monomer as corrosion inhibitors for A3 carbon steel in hydrochloric acid solutions: Experimental and quantum chemical studies, Colloids and Surfaces A: Physicochemical and Engineering Aspects 575, 57-65 (2019).

[44] Bin-Hudayb Nashwa S., Badr Entsar E., Hegazy M.A., Adsorption and corrosion performance of new cationic gemini surfactants derivatives of fatty amido ethyl aminium chloride with ester spacer for mild steel in acidic solutions, Materials 13, 2790-2817 (2020).

[45] El-Tabei A.S., Hegazy M.A., Bedair A.H., Sadeq M.A., Synthesis and inhibition effect of a novel Tri-cationic surfactant on carbon steel corrosion in 0.5 M H_2SO_4 solution, J. Surfact. Deterg. 17, 341-352 (2014).

[46] Han P., Chen C., Li W., Yu H., Xu Y., Ma L., Zheng Y., Synergistic effect of mixing cationic and nonionic surfactants on corrosion inhibition of carbon steel in HCl: experimental and theoretical investigations, J. Colloid Interface Sci. 516, 398–406 (2018).

[47] Ma X., Xu L., Wang W., Lin Z., Li X., Synthesis and characterization of composite nanoparticles of mesoporous silica loaded with inhibitor for corrosion protection of Cu-Zn alloy, Corros. Sci. 120, 139–147 (2017).

[48] Hegazy M.A., Azzam E.M.S., Kandil N.G., Badawi A.M., Sami R.M., Corrosion inhibition of carbon steel pipelines by some new amphoteric and di-cationic surfactants in acidic solution by chemical and electrochemical methods, J Surfact Deterg 19, 861–871 (2016).

[49] Han P., Li W., Tian H., Gao X., Ding R., Xiong C., Song L., Zhang X., Wang W., Chen C., Comparison of inhibition performance of pyridine derivatives containing hydroxyl and sulfhydryl groups:

experimental and theoretical calculations, Mater. Chem. Phys. 214, 345–354 (2018).

[50] Rakanta E., Zafeiropoulou T., Batis G., Corrosion protection of steel with DMEA based organic inhibitor, Constr. Build. Mater. 44, 507–513 (2013).

[51] Zeng L., Zhang G., Guo X., Chai C., Inhibition effect of thioureidoimidazoline inhibitor for the flow accelerated corrosion of an elbow, Corros. Sci. 90, 202–215 (2015).

[52] Hegazy M.A., Aiad I., 1-Dodecyl-4-(((3-morpholinopropyl)imino) methyl)pyridin-1-ium bromide as a novel corrosion inhibitor for carbon steel during phosphoric acid production, J. Ind. Eng. Chem. 31, 91-99 (2015).

الملخص العربى

تشييد ودراسة الخواص السطحية لمادة جديدة ذات نشاط سطحى كاتيونية ثنائية الشحنة ن,ن- (((2,2- (نفثالين-5,1 – دايل بس (أوكسى)) بس (أستيل)) بس (أوكسى)) بس (بروبان- 3,1 – دايل)) - بس (ن,ن- داى ميثيل دوديكان-1- أمونيوم) داى بروميد). تم تحديد كفاءة الصلب الكربونى من خلال طريقة الفقد فى الوزن والمعاوقة الكهروكيميائية للتحليل الطيفي والإستقطاب البوتنشيوديناميكى فى غياب ووجود المثبط. ووجد ان الكفاءة وقيم المعاوقة الكهربية لانتقال الشحنة تزداد بزيادة تركيز المثبط الكاتيونى وتقل بزيادة درجة الحرارة. اثبتت دوال الديناميكية الحرارية ان الكفاءة تحدث نتيجة امتزاز جزيئات المثبط على سطح الصلب الكربونى طبقا لمعادلة لانجمير. اظهرت نتائج الإستقطاب البوتنشيوديناميكى ان المركب المستخدم يعتبر مثبط مزدوج. اظهرت النتائج المعملية ان إمتزاز المثبط خليط من الإمتزاز الكيميائى والفيزيائى وتم تاكيد النتائج السابقة باستخدام الماسح المجهري الإلكتروني وطيف طاقة تشتيت الأشعة السينية حيث اظهرت تكون طبقة من المثبط على سطح الصلب الكربونى.